ION MICROPROBE ELEMENTAL ANALYSES OF IMPACT FEATURES ON INTERPLANETARY DUST EXPERIMENT SENSOR SURFACES.

Charles G. Simon
Institute for Space Science and Technology
Gainesville, FL 32609

Jerry L. Hunter, Jim J. Wortman, Dieter P. Griffis
North Carolina State University
Raleigh, NC 27695

ABSTRACT

Hypervelocity impact features from very small particles (<3 μm diameter) on several of the electro-active dust sensors utilized in the IDE experiment (LDEF Expt. No. A0201) were subjected to elemental analyses using an ion microprobe. After etching away a layer of alkali-rich carbonaceous/silicaceous surface contamination, low mass resolution elemental survey scans are used to examine impacted areas. Normalized high mass resolution two-dimensional positive ion elemental maps of the feature and surrounding area show the distribution and relative composition of the material. The location of the high purity sensor surfaces on the six primary sides of LDEF (rows 3, 6, 9, 12, space end, and earth end) provides a unique opportunity to further define the debris environment. We have applied the same analytical techniques to impact and contaminant features on a set of ultra-pure, highly polished single-crystal germanium wafer witness plates that were mounted on tray B12. Very little unambiguously identifiable impactor debris was found in the central craters or shatter zones of small impacts in this crystalline surface. Surface contamination ubiquitous on LDEF has greatly complicated data collection and interpretation from micro-particle impacts on all surfaces.

INTRODUCTION

The Interplanetary Dust Experiment (IDE) has yielded a wealth of spatio-temporal impact data for the first year of the LDEF orbit, including the first long-term direct evidence of the episodic nature of micro-particle impacts in low Earth orbit (LEO).[1] In order to extend the usefulness of this data set we have begun a systematic analysis of impactor residues in impact features on the high-purity sensor surfaces using scanning electron microscopy with energy dispersive x-ray spectroscopy (SEM/EDS) and secondary ion mass spectrometry (SIMS). Our ultimate objective is to produce a substantial data set on major element compositions of the smallest class of impactors (<3 μm). This will allow a statistical view of the manmade/natural micro-particle population ratio. Larger craters are also being examined during the course of the study and this data will be compared to other compositional data for similar sized impactors observed by other LDEF investigators.[2-4]

Impact craters on a set of high purity germanium witness plates mounted on tray B-12 have also been examined. Pre-flight surface contamination of these witness plates has complicated analyses of impact features. EDS and SIMS analyses of several contaminant features were recorded and a proposed sample clean-up procedure is presented. Primary beam shadowing effects compromise SIMS data on large, high aspect ratio craters (discussed below), but EDS analysis has identified tentative debris in all three large craters (60, 71 and 188 μm) found on Ge surfaces scanned to date.

In this paper we describe the impacted samples and analytical methodology in detail, and report on results from SIMS and EDS analyses of 15 impacts in IDE sensors from the leading and trailing sides of

LDEF (rows 9 and 3, respectively). Results are also presented of SIMS analyses of 13 impacts in Ge witness plates from tray B12. Half of these impacts were also analyzed with EDS. All but one of the impacts analyzed with SIMS had craters <~20 μm in diameter. An additional 11 impacts in Ge, nine that were <10 μm in diameter and two that were 60 and 188 μm diameter, were analyzed with EDS only. Dimensions and analytical results for all impacts analyzed to date are presented. Examples of SIMS two-dimensional elemental maps of several impact features are also presented. They show the usefulness of the technique in observing and correlating very small amounts of impactor residue and point out the problems associated with surface contamination and beam shadowing effects on a large crater in Ge.

The bar graph in Figure 1 shows the relative amounts of surface area for each micrometeoroid experiment on LDEF, the proposed range of impactor size chemical characterization, and the experiment locations on the spacecraft. This graph illustrates the potential for micro-particle impactor chemical characterization on impacts in IDE sensor surfaces compared to the other micrometeoroid experiments. The only other group currently using SIMS routinely to analyze impact craters (Zinner, et al., Expt. A0187-2) have no plans to characterize particles <10 μm in size.[5] The foil covered germanium capture cell experiment's major objective is the chemical and isotopic characterization of natural micrometeorites >10 μm in diameter, and the group is concentrating on analysis of impact features that formed when the capture cell foils were intact. However, the ultra-pure germanium capture cells in this experiment were exposed directly to the space environment for substantial times during the mission due to catastrophic failure of their thin-film covers. Thus, the large areas of pure germanium base plates (1.51 m^2 total) on rows 2, 3 and 8 should provide a significant source for micro-particle impact sites, albeit with variable and unknown time history. The SIMS procedures reported on in this paper were developed to analyze micro-particle impact sites on pure germanium and should be directly applicable.

Other LDEF investigators that have analyzed substantial numbers of impact craters have used SEM/EDS procedures to date.[3,4] Because of the inherent lower sensitivity of EDS versus SIMS, explained briefly below, and the small amount of impactor material (femto to picograms) expected to survive a micro-particle hypervelocity impact, most investigators have concentrated on analyzing larger impact features.

A notable exception is the work reported by Mandeville, et al., (Expt A0138-2, row 3) which includes identification of chondritic residues in ~10 micro-particle impacts (<5 μm diameter thin film penetration holes) analyzed so far out of a total of ~ 40 such micro-particle impacts identified on capture cell surfaces (0.2 m^2 total area).[4] However, analyses of off-impact areas had not been performed at the time the analytical data were presented. Our experience, and that of others in the LDEF community, has shown that surface contamination by alkali-rich silicaceous species is a significant problem for all LDEF surface analysis procedures.[2,3,6,7] This factor combined with the limited number of small craters in the A0138-2 experiment, and its location only on the trailing edge of the spacecraft limit the available statistics for determination of the average manmade/natural micro-particle population ratio from this experiment.

The A0187-2 experiment (Horz, et al.) had a large (~1m^2) collection surface on both the leading and trailing edge of LDEF and a substantial set of EDS analyses of impact craters >40 μm in diameter has been reported to date.[3,8] The row 11 collector surface is anodized Al alloy (99%) and the textured surface precludes easy identification of impact craters <~20 μm in diameter. Also, the materials impurity limits the ability to analyze small amounts of impactor residue. The row 3 experiment surface is 0.999% Au and has a somewhat smoother surface. It should be possible to identify smaller craters and analyze them using SIMS. Several samples of this surface are currently undergoing analyses in our laboratory.

Experiment A0023 was composed of ~1500 cm^2 of multi-foil capture cell surface area on the four primary LDEF sides ~700 cm^2 on the space end, and provides an excellent sample set for all impactor sizes up to ~1mm. McDonnell, et al., plan on a rigorous chemical analysis program after completing their primary mission of average flux determination.[9] The inherent impurity of the commercial foils and assembly materials used in the capture cells construction will complicate and may ultimately limit the investigators' ability to analyze residues from the smallest class of impactors (<3 μm). The use of SIMS may ultimately be

required to analyze significant numbers of micro-particle impact sites, and it is hoped that our laboratory's experience will be useful in this effort.

The largest area meteoroid experiment on LDEF, S0001, consisted of ~25 m^2 of chromic-anodized 6061-T6 Al alloy plates distributed on nearly all sides of the spacecraft.[10] This experiment is not represented in Figure 1 since it was not originally designed to permit chemical analyses of micro-particle impacts. The surface texture precludes identification of impact craters <~20 μm in diameter and the substrate impurities greatly complicate chemical analyses of impactor residues. However, the principal investigator, D. Humes, is currently collaborating with our laboratory to perform chemical analyses on selected residues in and around impact features >40 μm in diameter using SEM/EDS and SIMS.

The ultra-pure materials used in the fabrication of the IDE sensors and their location on all six LDEF primary sides provides a unique sample set for the determination of the manmade/natural micro-particle population ratio via chemical analyses. The smooth sensor surfaces and the impact signature (described below) greatly facilitate the location of micro-particle impacts. In addition, the activity record over the first year of LDEF's orbit permits identification of sensors that became inactive at specific times. In future studies this could allow segregation of impacts (and average fluxes) into before and after sensor failure times, thus providing another level of temporal characterization of the micro-particle population in LEO.

EXPERIMENTAL

The general experimental approach to sample analyses was as follows:

(1.) Perform a stereo optical survey at 100X magnification (Olympus 1000X stereo microscope) and
    photo-document impacts at low and high magnification for later identification in other instruments.
(2.) Perform SEM/EDS analyses of impact sites and surrounding areas.
(3.) Perform SIMS analyses of impact sites and surrounding areas.
(4.) Correlate all analytical data on each impact crater and tabulate relative abundance of elements found
    in craters and spall zones.

SIMS analysis was left to last since it is a destructive technique. The presence of a layer of alkali-rich silicaceous surface contamination complicated these analyses as discussed below. Also, the presence of pre-flight contamination on the germanium witness plates, in addition to the orbital contamination, greatly complicated analyses of impact sites on these surfaces. As the study progressed, EDS analyses of small impacts in Ge was discontinued since no detectable debris was observed with this technique in any of the small craters that were examined. Instead, SIMS analyses were performed after optical identification of the impact craters.

Description of Hypervelocity Impacts in IDE Sensors

The IDE sensors (Fig. 2) are 2 inch (5.08 cm) diameter Metal-Oxide-Silicon (MOS) capacitor structures. The detectors were formed by growing either a 0.4 μm or 1.0 μm thick silicon dioxide layer on a 250 μm thick, B-doped polished silicon wafer (>0.99999). The top metal contact was formed by physical vapor deposition of ~1000Å of aluminum(>0.9999). Aluminum was also vapor deposited on the backside of the wafers to form the contact with the p-type Si substrate. Gold wires were then bonded to the front and back Al layers and used to connect the detectors to the circuits. The completed wafers (IDE detectors) were then mounted on Al frames by bonding the backsides with silicon RTV. A total of 459 sensors were flown on the six primary sides of LDEF; 60% had 0.4 μm thick insulator layers and 40% had 1.0 μm thick insulator layers.

The IDE capacitor detectors were placed in an electrical circuit that supplies a positive bias to the top Al electrode and a negative bias to the bottom electrode/Si-substrate. The detector operates by discharging the charge stored in the capacitor when impacted by a particle with sufficient mass and energy to cause the thin silicon dioxide layer to fail. The level of the stored charge is chosen to allow sufficient energy during discharge to vaporize a small area of the top Al electrode around the impact point. The typical diameter of this vaporized discharge zone is 50-70 μm and is directly related to the applied voltage/stored charge and the thickness of the Al layer. Once the discharge takes place the capacitor circuit recharges within a maximum of 3-4 seconds if the applied voltage is maintained. The impact event is recorded electronically by monitoring this recharge current. The recharge time is dependent on the rate at which current is allowed to flow to the detector.

The morphology of an impacted region can be seen in Fig. 3. Typically there is the impacted area at or near the center of the feature surrounded by a 25-35 μm wide area of damaged insulator (SiO$_2$), and a 50-70 μm wide zone where the Al has been vaporized. There is also a rim of melted Al which defines the extent of the vaporization zone. These morphological features greatly facilitate the location of micro-particle impacts on active sensor surfaces and also serve to distinguish impacts that occurred when the sensor was inactive. The smooth-bottom, low aspect central craters in the impact sites that occurred on active 1.0 sensors have a minimum diameter of ~11 μm. Since submicron particles are capable of triggering the sensors (~0.5 μm diameter particle for the 1.0 sensor and ~0.2 μm particle for the 0.4 sensor), the minimum crater diameter is interpreted as being a function of the specific electrode surface area required for electron flow to occur under the applied voltage. It is suspected that the negative potential field of the Si electrode may enhance capture of positive ions produced in the impact/sensor-discharge plasma plume. However, insufficient empirical data from ground based simulations of this phenomenon has been collected to date to unambiguously identify an enhanced ion collection effect.

It is not known at this time what maximum size impactor would inactivate a sensor, but theoretically even a broken sensor wafer should still be active on the areas attached to the electrode leads. A substantial number of large impact craters (> 0.5mm diameter) were observed on IDE sensor surfaces. An accounting of the largest impacts on those sensors that were still active when LDEF was retrieved should provide a limit for this value. Central crater and Al vaporization zone diameters are reported for all impacts subjected to residue analyses.

During the manufacture of the IDE sensors, particulate contamination and defect sites in electrode interfaces necessitated the "clearing" of sensors before mounting on the spacecraft. This was accomplished by activating the sensors at a potential higher than the flight potential and causing the contaminant and defect sites to discharge and clear themselves. Photographic records were then made of each sensor which allows an accurate accounting of all pre-flight discharge areas. Sensors varied greatly in their degree of susceptibility to pre-flight discharges. SEM and SIMS analyses of four pre-flight discharges revealed the presence of contaminants (from dust particles or tool marks) and markedly different morphology than in-flight discharges. To date we have not analyzed a true "blank" discharge, but we have plans to generate several blanks on reactivated flight sensors using a pulsed laser and subject them to SIMS analyses. The two 1.0 sensors selected for impact analyses in this study were characterized as "good" and had few pre-flight discharges.

Description of Hypervelocity Impacts in Germanium Witness Plates

Twelve 1.25 inch (3.175 cm) diameter, 250 μm thick semiconductor device quality single crystal Ge wafers were glued to Al plates with silicone RTV, mounted on tray B12, and exposed to the orbital environment during the entire mission. These wafers were intended to serve as witness plates both for hypervelocity impacts and surface contaminants. However, during optical examination it was noted that the surfaces of these wafers were covered with solid contaminants with condensate rings at a density of ~400 features (>10 μm diameter) per cm^2. Optical surveys of three other similar sized witness plates (one zirconia and two silicon) mounted adjacent to the Ge witness plates revealed only 10-27 similar contaminants per cm^2

on these surfaces. This is taken as conclusive evidence that the majority of the contaminants on the Ge wafers were deposited before they were mounted on the spacecraft with the other witness plates. Auger, EDS and SIMS analyses of dozens of these contaminant features showed a dominance of alkali-chlorides, hydrocarbons, Mg, Si, Ca, S, Ti, some Fe, and very little Al.

The contamination problems are complicated further by the morphology of the impact features in the Ge substrates. A typical impact feature has a high aspect central crater (or shatter zone if larger than ~10 μm diameter), an extremely jagged inner spall zone about twice the diameter of the crater, an outer spall zone with a maximum dimension about four times the crater diameter, and a fracture zone that spans a distance equal to 5-10 times the crater diameter (Fig. 4). About half of the craters < 10 μm in diameter did not have an outer spall zone. The jagged central shatter zones of the larger craters restricted the usefulness of SIMS analyses, as discussed below.

The high level of pre-flight particulate contamination combined with the alkali-rich silicaceous surface contamination layer deposited in orbit have greatly complicated instrumental analyses of impact sites on these surfaces. We have not cleaned the surfaces to date, beyond nitrogen blow down, prior to their introduction into the SIMS instrument. Careful examination of two-dimensional elemental concentration maps was required to identify residue located in craters and spall zones. Even with these precautions, the identification of debris must be considered tentative until more stringent sample preparation procedures are instituted. Our current plans are to use the alcohol/water surface cleaning procedures utilized by investigators that examined impact craters on Apollo spacecraft windows[11,12] to clean one Ge wafer and reanalyze several impacts that showed high concentrations of residues within impact craters. These craters should have significant material remaining despite the destructive nature of SIMS analysis.

SEM/EDS Analyses

Energy dispersive x-ray spectroscopy is based on the measurement of the characteristic X-rays from materials excited with an energetic electron beam. The EDS used in this study allowed the detection of all elements with Z > 10 (Ne), with minimum detection sensitivities for the various elements ranging from ~0.1% to >1.0% atomic concentration. All experiments were performed on an Hitachi S-530 scanning electron microscope equipped with a Tracor-Northern TN5500 EDS. SEM micrographs were recorded of the impact features and EDS spectra were recorded of various areas within the impact feature (central crater and spall zone) in both area and spot mode. All SEM micrographs were recorded with an accelerating voltage of 5 KV and EDS spectra were recorded at both 5 KV and 15 KV. Substrate background EDS spectra were also recorded at 5 KV and 15 KV away from any impact features and obvious surface particulate contamination.

SIMS Analyses

In secondary ion mass spectrometry an energetic ion beam (1 to 20 KeV) is directed toward the sample to be analyzed. The sample surface is eroded by sputtering, and the ionized, sputtered species (atoms or molecules) are extracted into a mass spectrometer where they are separated according to their mass/charge ratio and then counted or imaged. The advantages of SIMS include: [1] detection limits of ppm to ppb for most elements, [2] the ability to detect all species (including H), [3] the ability to record two-dimensional secondary ion images, and [4] excellent depth resolution (<100 Å). The major disadvantages are: [1] SIMS is an inherently destructive technique due to the sputtering process, [2] quantification is not straight-forward due to the complicated secondary ion formation processes involved, [3] large topographic features can lead to false contrast, and [4] trace contaminants complicate interpretation of data from unknown samples.

The primary ion beam impacts the sample at ~30° from normal for the primary ion energy used in this study (15 KV). Figure 5 shows the shadowing effect caused by sputtering at this angle. The sidewalls of a high aspect ratio (depth/width) feature can shadow the primary ion beam from the bottom of the deep feature, thereby preventing sputtering from this area. This is of particular importance when trying to record signals from the bottom of deep craters with jagged sidewalls. (Smooth sidewalls can actually act to focus

the ion beam into the crater, but spatial resolution within the hole is lost due to scattering.) All of the larger impacts (>20 μm) found in the Ge witness plates had central shatter zones instead of smooth walled craters (see Fig. 4b for an example). This shadowing effect and poor secondary ion extraction from these deep, jagged features resulted in a greatly reduced signal from the crater bottom.

The main advantage of SIMS, its excellent sensitivity, can be a disadvantage if sample substrates are not of sufficient purity because non-detectable amounts of elements for other techniques (i. e. EDS, Auger) can give rise to large signals in SIMS. Interferences can also arise from molecular ions having the same nominal mass as the element of interest. These interferences can be resolved in most cases by operation of the ion microscope in the high mass resolution mode, which allows the resolution of 2 species differing by only a few parts per thousand in mass. A particular interference of interest is the Si_2^+ secondary ion (mass = 55.95386 amu) interfering with Fe^+ (mass=55.93494 amu). A mass resolution of 2956 m/Δm, easily achievable in the IMS-3f, is required to separate this interference.

All experiments were performed on a CAMECA IMS-3f Ion Microscope equipped with oxygen and cesium primary beams. The IMS-3f is a double focussing magnetic sector SIMS instrument capable of achieving mass resolutions up to 10,000 m/Δm. It is also a stigmatically imaging ion microscope capable of imaging the elemental distribution with ppm sensitivity and ~1μm lateral resolution.

All data were taken with a 15 KeV O_2^+ primary ion beam. Background positive ion mass spectra were recorded of the surface away from impact features and obvious contamination at 50 nA primary ion current. After recording a mass spectra from 0-200 a.m.u., a depth profile was acquired at 500 nA primary current while monitoring C^+, Na^+, Si^+ and Ca^+ in order to assess the time required to sputter through the layer of surface contamination.

A final protocol was developed to record SIMS data of impact features on high purity LDEF surfaces. Impacts examined during the development of the protocol did not always adhere to this final form and deviations are detailed in the next section. A sample cleaning protocol based on the results of this study and intended to minimize contamination interferences is currently in the development stage. Unless otherwise noted, the following protocol was used to record SIMS data of impact features:

(1.) A Mass spectrum from 0-200 a.m.u. was taken of the central impact crater and associated discharge zone (for impacts in IDE sensors) or spall zone (for impacts in Ge witness plates) at 50nA primary current. This mass spectrum was energy filtered in order to minimize molecular interferences with elemental ion signals.[13] During this portion of the analysis <200Å of material were consumed. In practice, the reproducibility of these initial mass spectra on each substrate lead to the decision to delete this step after several features had been analyzed on each different surface.

(2.) A depth profile was recorded at 500nA primary ion current while monitoring the secondary ion signals of O^+, Si^+, Ca^+ and Na^+ in order to assure that the surface contamination layer was removed. The amount of surface material removed during this process was dependent on the thickness of the silicaceous contaminate layer and varied from hundreds to thousands of angstroms on the various substrates analyzed. Duration of the depth profile was also based on a similar profile recorded for a background area on the substrate in the vicinity of the impact sites.

(3.) A second mass spectrum was recorded of the sputtered area. Based on the results of this spectrum, and the expected compositions of manmade debris and natural micrometeoroids, positive ion images were recorded at 500 nA primary ion current for some or all of the following species: C^+, O^+, Na^+, Mg^+, Al^+, Si^+, K^+, Ca^+, Ti^+, Cr^+, Fe^+, Ni^+, Cu^+, Zn^+, Ge^+, Ag^+ and Au^+. [No images were recorded for Zn^+, Ge^+, Ag^+ and Au^+ on most IDE sensor surfaces Also, Na^+ images were not recorded for most impacts in the leading edge sensor (No. 293). Current protocol for impacts in IDE sensors includes high mass resolution analyses for all of the

positive ions listed, except Ge$^+$.] During this portion of the analysis <2000Å of material were consumed.

(4.) All secondary ion images were semi-quantitatively scaled based on the secondary ion yields for the elements of interest being sputtered from a pure target (i.e. Si or Ge).[16] Results were then tabulated in terms of relative abundance and location of elements found in and around the impacts.

In order to investigate the possibility of the alkali rich carbonaceous/silicaceous layer being non-uniformly sputtered from the crater bottom and spall areas in impacts in Ge due to the large topography differences, a depth profile was recorded at 500nA for ~25 minutes on one impact feature (Ge2A-15). Under these conditions the contaminate layer was removed from the smooth background area of the Ge wafer in 9 minutes, as evidenced by the precipitous drop and leveling out of the Si$^+$ and alkali positive ion signals. However, after 3 minutes the Si$^+$ and Na$^+$ signals from the impact site leveled off at ~100X the background concentration and remained at this intensity until the depth profile was terminated (Fig. 6). This result leaves open the possibility of contaminate contribution to ion signals within the impact areas on Ge substrates due to differential sputtering effects. The significantly lower initial signals from Si and Ca over the impact site could be the result of removal of the contaminant layer by the impact event followed by redeposition of a thinner layer.

The frequent close proximity of contaminant spots that contained many or all of the elements detected in the impact feature on Ge precludes unambiguous identification of impactor residues. These complications, along with the small surface area of the Ge witness plates and their location on only one side of LDEF, have precipitated the decision to concentrate future SIMS analyses on impact features in the IDE sensors. There are similar contamination problems with these samples, but to a significantly lesser degree.

RESULTS AND DISCUSSION

This preliminary study focused on development of analytical protocols and identification of associated analytical problems. Surface contamination proved to be the most significant factor in limiting the usefulness of SIMS data collected from impact features on both the IDE sensor surfaces and the Ge witness plate surfaces. The morphology of the impacts in Ge and the high density of non-flight surface contaminants severely restricts the usefulness of the data collected from these surfaces. The experience gained in this study has resulted in development of appropriate SIMS instrumental and data handling protocols for analysis of micro-particle impact features on IDE sensor surfaces and other high purity substrates. These protocols can now be used to focus on minimization of interferences from contamination, and gaining an understanding of the impact phenomenon in active IDE sensors as it relates to the deposition and recovery of impactor residue. These issues are addressed below in the discussion of the data sets and their specific limitations.

Analytical Results for Impacts in IDE Sensors

The small number of impacts analyzed on two leading and trailing edge IDE sensors (six and nine impacts, respectively) during this development phase study provided sufficient data to allow identification of the limitations of this sample set based on our current understanding of the impact phenomenon in the active sensors and the uncertainty due to interferences from contamination. The effects of these issues will be examined in three ways. First, loose particles and/or soluble debris will be removed from sensor surfaces with three cycles of rinsing and light wiping with lint-free soft cotton using high purity water, methanol and acetone followed by vacuum bakeout at 325K. Hypervelocity impactor melt residues and ion implanted materials should not be removed by this process. Little, if any, of the UV polymerized silicaceous contaminant layer is expected to be removed by this process. Second, several "blank" discharges on an active flight sensor and on an active non-flight sensor will be produced using a pulsed laser and analyzed

with SIMS to discern the distribution of integral and flight-accumulated contaminants. Third, several Fe/C micro-particle hypervelocity impacts on an active flight sensor and on an active non-flight sensor will be produced using an accelerator and analyzed with SIMS in order to discern the distribution of the projectile material and its level of intermixing with integral and flight-acccumulated contaminants. After these studies are performed, a decision can be made on the usefulness of performing SIMS analyses on a statistically significant number (>100) of micro-particle impacts in leading and trailing edge sensors.

Six impacts randomly selected from a total of 200 in-flight discharges identified on a leading sensor (45.6 cm² total area), No. 293, and nine impacts randomly selected from a total of 25 identified on a trailing edge sensor, No. 300, were analyzed with EDS and SIMS. Both sensors that were active during the entire mission and the ~9/1 ratio of leading/trailing edge impacts was in the same range as the ratio for larger impactors (craters >0.5 mm diameter) observed by the LDEF Meteoroid and Debris Special Investigation Group.[10] No elements other than Si and Al were observed in EDS analyses and only Si was found in area analyses of all central craters. Spot analyses of numerous melt blebs, droplets and rims showed only Si and/or Al.

SIMS analysis showed that significant amounts of Na, Mg, K and Ca were present in the silicaceous surface contamination layer. (Ca was also present at a >10 ppm concentration throughout the Al layer on sensor 293, as evidenced by depth profile.) Due to local variations of the composition and thickness of the layer, it was impossible to be sure if the layer was etched away from the entire analysis area before ion images were taken. For example, in four of the leading edge impacts, and two of the trailing edge impacts, Ca surrounds the entire feature but is not present in any of the central craters. In fact, Ca was not found in the central craters of any of the 15 impacts examined. These observations increase the confidence that the surface layer was effectively etched away from at least the central crater portions of the features, which are considered the most critical area of the features for identifying impactor residue.

Table 1 lists the SIMS analytical results for material found in and around impact sites in order of approximate (within one order of magnitude) decreasing relative elemental abundances. Results for Al and Si (the substrate materials) are not listed, but no high concentrations of Al were noted in any of the central craters. Low concentrations of Al (<~1000 ppm) would not be visible due to dynamic range limitations of the detector. Only positive ions were analyzed since the vast majority of the elements of interest have a much greater positive ion yield compared to their negative ion yields. Notable exceptions are F, S and Cl, which were not looked for in this phase of the study because of the complexity of switching the Cameca IMS-3f Ion microscope from positive to negative ion analysis mode. In a comprehensive analytical study of large numbers of micro-particle impacts negative ion analyses of selected residues could help to identify chloride salts, fluorocarbon debris, and Fe meteorites, which usually have high S content.

Residues were found in four distinct areas (refer to Fig. 3), [1] the central crater, [2] the discharge area or, or Al vaporization zone, [3] the slightly raised Al melt rim that encircles the discharge area, and [4] the area around the outside of the feature. SIMS analysis areas were 150 µm in diameter with the impact feature positioned near the center. The diameters of the central craters and discharge areas are also listed with the results.

The leading edge sensor, No. 293, had a thicker layer of vapor deposited Al on its surface than the trailing edge sensor. Discharge zone diameters ranged from 59-79 µm in diameter with no apparent relation to the diameter of their respective central craters. Na⁺ was looked for in only one feature on this sensor, No. 293-2, and was not observed. Impact No. 293-1 had significant amounts of K, Mg and Fe in roughly equal proportions in the 17 µm diameter central crater, no residue in the discharge area, a small spot of residue with Ca > Fe in the discharge rim and no significant residue around the outside of the feature. Impact No. 293-2 had a significant amount of Mg and K residue in the 24 x 31 µm central crater with Mg > K. Residue consisting of Fe > Ca was found in the discharge area, and Fe > Mg and Ca with a trace amount of K were found distributed in a ring throughout the feature's discharge rim. Ca and Fe were seen all around the outside of the feature. Impact No. 293-3 had significant amounts of K only its 18 µm central crater. Fe>>K was found in the discharge area, and Fe > Mg, Ca > K was found distributed in a ring

536

throughout the feature's discharge rim. Ca and Fe and a trace of K were present all around the outside of the feature.

Impact No.293- 4 was unique in that it had a very high concentration of Fe in its 12 μm central crater along with a much lesser amount of Mg. Unnormalized positive ion images of Mg, Al, Si, K, Ca and Fe are shown in Fig.7. Some Fe was also present in the discharge area close to the crater associated with a lesser concentration of K. A ring of residue composed of Fe, Mg >> K was present in the discharge rim and Ca was found all around the outside of the feature. This feature has been identified as a candidate for reanalysis after wet cleaning of the sensor surface.

Impact features Nos. 293-5 and 293-7 had no detectable residue in their respective 22 x 28 μm and 12 μm central craters or in their discharge areas. Number 293-5 did have a ring residue consisting of C > Mg, K in the discharge rim and a spot of Fe>Ni>Mg ~40 μm away from the feature. Ca was also present all around the outside of the feature. The only residue found near feature No. 293-7 was a loose particle of Fe>Mg, Cr > Ni with traces of K and Ca (a typical stainless steel composition) found just outside the discharge rim and identified in the SEM.

In summary, four of the six impacts analyzed on the leading edge sensor had residues in their central craters composed of K and/or Mg and/or Fe. Residue in one crater consisted of K only, one consisted of Mg and K, one consisted of Fe with a small amount of Mg, and one consisted of Mg, K, and Fe. Four of the six features had rings of residue in their discharge rims consisting of Mg, Ca and Fe, with lesser amounts of K in two cases, Mg and Fe with a small amount of K in one case, and C with lesser amounts of Mg and K in one case. These same four features all had substantial amounts of Ca in the analysis areas surrounding them.

The trailing edge sensor, No. 300, had a thinner layer of vapor deposited Al (positive electrode for the sensor) than sensor 293. Discharge zone diameters ranged from 44-60 μm in eight nominal impact sites. All of the impacts had moderate amounts of C spread over the area around the features and six of the nine impacts had a concentrated ring of C in the features' rims. Ca surrounded only two of the impact features, which is an indication that the Ca contamination in the bulk of the Al film is not homogeneously distributed.

Impact feature No. 300-1 on this sensor was an exception. It was the result of a large particle impact that left a 36 x 54 μm central crater with a spall zone that had a maximum dimension of 138 μm (refer to Fig. 3b). The diameter of the residual discharge rim was 91 μm. Some Mg was present in the central crater and there were two spots of residue in the spall zone composed of Fe and Ti in one case and Na, Mg, K and Ca in the other. No significant debris was found in the immediate vicinity of the large impact's borders.

Impact No. 300-2 had some Na in the 13 x 18 μm central crater, nothing in the discharge zone, and a ring of concentrated C in the discharge rim. There was also a spot of Na, Mg, K, Ca residue in the analyzed area outside of the discharge rim. Impact No. 300-3 had some Na, Mg, K residue in the 12 μm diameter central crater, nothing in the discharge zone, a ring of concentrated C in the discharge rim, and a Ca, Fe > Mg spot with traces of Na and K outside the discharge rim.

Impact Nos. 300-4 and 300-6 had no residues in their respective 13 and 10 μm diameter central craters, nor in their discharge zones. Both features had a ring of concentrated C in the discharge rim. A chloride salt crystal with significant amounts of Na, K, Ca, Mg, Fe and Ti was identified with the SEM/EDS in the discharge zone of impact 300-4. This impact has been identified as a candidate for reanalysis after wet cleaning of the sensor surface.

Impact No. 300-5 had some Na, Mg, K residue in its 11 μm diameter central crater, nothing in the discharge zone, a ring of concentrated C in the discharge rim along with a spot of high concentration C and Fe with lesser amounts of Na, Mg, and Cu. This was the only residue containing Cu identified in any of the 15 impacts examined on the IDE sensors, and a Ca, Fe > Mg spot with traces of Na and K outside the discharge rim.

Impact No. 300-7 had a residue consisting mostly of Ti with a substantial amount of Na and a trace of K. Nothing was seen in the discharge zone, but a ring of C and Na was observed in the discharge rim. This was the only example of Ti residue found in a central crater in the 15 IDE impacts, but impact No. 300-8 had a significant amount of Ti in its discharge zone along with Na, Mg, K and Ca. This feature also had a residue of Na and K in its 12 μm diameter central crater, a ring deposit of Mg, Ca and Ti in its discharge rim, and a substantial amount of Ca all around the outside of the feature. Impact No. 300-9 had a residue of only Fe in its 11 mm diameter central crater, nothing in the discharge zone or discharge rim, and one spot Na and K outside the discharge rim.

In summary, 7 out of 9 impact features analyzed on the trailing edge sensor had residues in their central craters. Two of the residues consisted of Na, Mg and K, one consisted of Ti with a lesser amount of Na and a trace of K, one consisted of Na and K, one consisted of Na only, one consisted of Mg only, and one consisted of Fe only. Five of the impacts had concentrated C rings in their discharge rims, and one of these rings also had Na distributed throughout it. A sixth discharge rim ring consisting of Mg, Ca and Ti was observed around one feature that also had these elements present in its discharge zone along with Na and K. Two of the nine impacts also had substantial amounts of Ca all around the outside of the features. (This compares with four out of six impacts on the leading edge sensor that were surrounded by Ca deposits.)

Analytical Results for Impacts in Ge Witness Plates

A total of 36 hypervelocity impact craters were identified in the 100X optical scan (and verified at up to 1000X) of two Ge witness plates (15.8 cm^2 total area). Diameters of the central crater diameters ranged from 2.5-188 μm (see Table 2). The five largest craters were 188, 71, 60, 30 and 22 μm in diameter. There were another 10 craters in the 10-20 μm size range and 18 in the 5-10 μm size range. The other three craters found in the optic scan were <5 μm in diameter.

SEM/EDS analyses were performed on 17 of the impacts, including 4 of the 5 largest ones, the three smallest ones, and about half of the mid-sized ones. The three largest craters showed the presence of impactor residue in two (both classified as "manmade" particles), and suspected contamination (silicon RTV) in a third. The lack of any impactor residue observed with EDS in any of the other craters agrees with observations by Amari, et al. for small primary impacts in Ge.[2] However, the EDS analyses performed in this study were generally limited to signal collection from the entire central crater areas at 5 KV and 15 KV, and cannot be considered exhaustive.

A 71 μm crater had high concentrations of Al and Si detected with EDS only in the central crater. SIMS analysis of this crater showed only a trace of Ca and Fe in the spall zone. No ion signals other than Ge$^+$ were seen from the central crater. This exemplifies the problems of beam shadowing discussed above.

A second large crater, 60 μm crater had a residue of Al and Si with lesser amounts of Cu, Zn and S identified with EDS. No SIMS analyses were performed on this impact. In both cases there was no visible evidence of contamination present in the craters and the residue was in the form of melt blebs. It is probable that the impactors responsible for these craters were of manmade origin.

Twelve additional craters, ranging in size from 6-22 μm, were analyzed with SIMS. Results are presented in Table 3 along with notes about contaminant features observed in the vicinity of impact sites. Because of the substantial contamination issues, discussed above, and the unknown extraction efficiencies of ions from the deep,jagged central craters present in most features, the discussion of the analytical results at this time would be completely ambiguous. Readers are cautioned on drawing conclusions about impactor origins based on these data. The data are presented for completeness with the previously mentioned caveats in full effect.

538

SUMMARY

In this preliminary study analytical protocols have been developed for sample handling and SIMS analyses of hypervelocity impact features on IDE sensors and other high purity substrates. Associated analytical problems have been identified and possible solutions proposed. Surface contamination proved to be the most complicating factor in interpretation of SIMS data. Distribution of integral and on-orbit accumulated contamination will be addressed by inducing several hypervelocity impacts with particles of known composition and several "blank" discharges on active flight and non-flight sensors using an accelerator and a pulsed laser, respectively. SIMS analyses of these features should provide significant insight into this issue and permit useful interpretation of data collected to date and in future analyses.

ACKNOWLEDGEMENTS

REFERENCES

1. J. D. Mullholand, S. F. Singer, J. P. Oliver, J. L. Weinberg, W. J. Cooke, P. C. Kassel, J. J. Wortman, N. L. Montague and W. H. Kinard: IDE spatio-temporal impact fluxes and high time-resolution studies of multi-impact events and long-lived debris clouds. First LDEF Post-Retrieval Symposium. NASA CP-3134, 1992.

2. S. Amari, J. Foote, E. K. Jessberger, C. G. Simon, F. J. Stadermann, P. Swan, R, Walker and E. Zinner: SIMS analysis of extended impact features on LDEF experiment A0187-2. First LDEF Post-Retrieval Symposium. NASA CP-3134, 1992.

3. F. Horz, R. P. Bernhard, T. H. See, J. Warren, D. E. Brownlee and M. Laurance: Preliminary results from the Chemistry of micrometeoroids experiment (A0187-1). First LDEF Post-Retrieval Symposium. NASA CP-3134, 1992.

4. J. C. Mandeville: Study of meteoroid impact craters on various materials (A0138-1) and Attempt at dust debris collection with stacked detectors (A0138-2). First LDEF Post-Retrieval Symposium. NASA CP-3134, 1992.

5. E. Zinner, H. Kuczera and N. Pailer: Simulation experiments for the chemical and isotopic measurements of interplanetary dust on LDEF. 13th Lunar and Planetary Science Conference Abstracts. 1982.

6. B. A. Stein (editor): *Preliminary Report on LDEF-Related Contaminants.* (Available through NASA/LaRc LDEF Office) 1990.

7. B. A. Stein and G. Pippin: Preliminary findings of the Materials Special Investigation Group. First LDEF Post-Retrieval Symposium. NASA CP-3134, 1992.

8. R. P. Bernhard, D. E. Brownlee, M. R. Laurance, W. L. Davidson and F. Horz: Survey-type analyses of projectile residues on select LDEF surfaces and craters. 22nd Lunar and Planetary Science Conference Abstracts, 1991.

9. J. A. M. McDonnell and K. Sullivan: Foil perforation particulate impact records on LDEF MAP A0023: Incident mass distributions. First LDEF Post-Retrieval Symposium. NASA CP-3134, 1992.

10. T. See, M. Allbrooks, D. Atkinson, C. Simon and M. Zolenski: *Meteoroid and Debris Impact Features Documented on the Long Duration Exposure Facility.* NASA/JSC Publication #24608, 1990.

11. B. G. Cour-Palais: Results of examination of the Skylab/Apollo windows for micrometeoroid impacts. Proc. 10th Lunar and Planet. Sci. Conf., p. 1665-1672 (1979).

12. U. S. Clanton, H. A. Zook and R. A. Schultz: Hypervelocity impacts on Skylab IV/Apollo windows. Proc. Lunar and Planet. Sci. Conf., p. 2261-2273 (1980).

13. R. G. Wilson, F. A. Stevie and C. W. Magee: *Secondary Ion Mass Spectrometry,* p App.E.11 and App.E.17 (J. Wiley and Sons) 1989.

Table 1. Summary of morphology and SIMS analytical data for impacts on IDE Al/Si sensor surfaces. SIMS analyses were for positive ions only. Results for Al and Si are excluded. No impactor debris was identified in any features using EDS. Small letters denote the presence of only a trace concentration of the species. Sequentially listed elements were present in the same area.

Impact No.	Crater dia.(μm)	Discharge Area dia.	Relative Abundance of Elements Found in			Notes
			Crater	Discharge Area	Rim	

Sensor 293 (row 9, leading edge)

Impact No.	Crater dia.(μm)	Discharge Area dia.	Crater	Discharge Area	Rim	Notes
1	17	79	Mg,K,Fe	-	Ca>Fe (spot)	
2	24 x 31	74	Mg>K	Fe>Ca	Fe>Mg,Ca>k (ring)	(Ca,Fe) all around feature
3	18	68	K	Fe>>K	Fe>Mg,Ca>K (ring)	(Ca,Fe>>k) all around feature
4	12	70	Fe>>Mg	Fe>K	Mg,Fe>>K (ring)	Ca all around feature; Fe in crater is high conc. spot
5	22 x 28	59	-	-	C>Mg,K (ring)	(Fe>Ni>Mg) spot away from feature; Ca all around
7	12	65	-	-		(Fe>Mg,Cr>Ni>k,ca) particle just outside feature

Sensor 300 (row 3, trailing edge)

Impact No.	Crater dia.(μm)	Discharge Area dia.	Crater	Discharge Area	Rim	Notes
1	36 x 54	91	Mg	Fe,Ti and Na,Mg,K,Ca spots in spall zone		large impact, 138 μm wide asymmetric spall zone
2	13 x 18	55	Na	-	C (ring)	(Na,Mg,K,Ca) spot outside of feature
3	12	44	Na,Mg,K	-	C (ring)	(Ca,Fe>Mg>>Na,K) spot outside of feature
4	13	46	-	-	C (ring)	(Na,Mg,K,Ca>Fe,Ti) particle next to crater identified as salt crystal in SEM/EDS
5	11	43	Na,Mg,K	-	C (ring);C,Fe> Na,Mg,Cu (spot)	
6	10	39	-	-	C (ring)	
7	12	46	Ti>Na>>k	-	C>Na (ring)	
8	12	50	Na,K	Na,Mg,K,Ca,Ti	Mg,Ca,Ti (ring)	Ca all around feature
9	11	60	Fe	-	-	(Na,K) spot outside Ca all around outside

Table 2. Summary of germanium witness plate impact feature dimensions and analyses. All impacts identified during a 100X optical scan are listed. Ratios of inner and outer spalls (not including attached chips or fracture zones) to crater dimensions, S$_I$/C and S$_O$/C, are for maximum spall dimensions and average crater diameters. Craters marked with an asterisk (*) and/or a triangle (Δ) were analyzed for impactor debris using SIMS and/or EDS, respectively.

Impact I.D.	Crater dia. (μm)	Inner Spall dia. (μm)	Outer Spall dia. (μm)	S$_I$/C	S$_O$/C	Tentative Impactor Debris Identified
Ge2A-						
1	30	50	75 x 88	1.67	2.93	-
2	6	8	10 x 13	1.33	2.17	-
3	8	15	22 x 25	1.88	3.13	-
Δ4	7	20	26 x 45	2.82	6.36	no
5	10	18	28 x 34	1.80	3.40	no
*6	7	14	-	2.00	-	yes
*7	8	15	28	1.88	3.50	yes
8	10	22	37 x 46	2.20	4.60	-
Δ9	7 x 10	15	-	1.83	-	no
Δ10	6	14 x 16	-	2.38	-	no
*12	6	14	-	2.33	-	yes
*13	8	20	24 x 26	2.50	3.25	yes
14	7	13	-	1.86	-	-
*15	8	16	18 x 22	2.00	2.75	yes
16	8	18	22 x 35	2.25	4.38	-
*Δ17	71	167	354 x 379	2.35	5.34	yes
*18	17	27	44 x 59	1.59	3.47	yes
19	11	27	-	2.45	-	-
Δ20	188	600	1070	3.19	5.69	yes
Δ21	2.5	5.0	-	2.00	-	no
Ge2B-						
1	12	24	27 x 42	2.00	3.50	-
*Δ2	14	32	48	2.29	3.43	yes
*Δ3	6	17	19 x 35	2.83	5.83	yes
*Δ4	17	41	80	2.41	4.71	yes
5	7	18	-	2.53	-	-
*6	15	38		2.33	5.87	yes
Δ7	60	143	293	2.39	4.89	yes
*Δ8	15	35	73 x 88	2.33	5.87	yes
Δ9	6	10	13 x 17	1.67	2.83	no
10	6	10 x 14	-	2.66	-	-
Δ11	3.2	8	-	2.41	-	no
Δ12	6	13	-	2.17	-	no
*Δ13	22	55	120	2.50	5.45	yes
Δ14	8	17 x 19	-	2.39	-	no
15	15	40	-	2.67	-	-
Δ16	4.5	11	13 x 18	2.44	4.04	no

Table 3. Summary of elemental analysis data for tentative hypervelocity impactor debris identified in impact features in germanium witness plates mounted on LDEF tray B12. Listed species were found in the craters and/or spall zones. SIMS analyses were for positive ions only. Small letters denote the presence of only a trace concentration of the species. Sequentially listed elements were present in the same area. Readers are cautioned on drawing conclusions about impactor origins based on these data due to unresolved contamination interferences.

| Impact No.	Crater dia.(μm)	Analysis Method	Relative Abundance of Elements Found in Crater or Spall Zone	Notes
Ge2A-				
6	7	SIMS	Al,K>Na,Mg,Si,Ca,Fe,Zn>Ti,	
7	8	SIMS	C,Na,K,Ca>Mg,Al,Ni,Fe,Cu	
12	6	SIMS	Na,Mg,Si,K>Ca	(Na,K,Ca,Ti,Zn,Cu) spot just below impact site
13	8	SIMS	Si>Na,Mg,Al,K,Fe	(C,Na,Al,Si,K,Ca>Fe) spot near impact site
15	8	SIMS	Na,Mg,Fe	
17	71	EDS	Al,Si	In central shatter zone only. Not seen in SIMS
17	71	SIMS	Ca,Fe (only in spall zone)	(Na,Mg,Al,Si,K,Ca,Fe) spots all around impact site
18	17	SIMS	Si,Fe>Mg	(C,Na,Mg,Al,Si,K,Ca>Ti,Cr) spot in vicinity of impact site.
Ge2B-				
2	14	SIMS	Si>Na	(Na,Fe,Cu) spot near impact site. Nothing seen in EDS.
3	6	SIMS	Na,Mg,Si>K,Al	Nothing seen in EDS.
4	17	SIMS	Mg>Na (covers impact feature and ~1/2 of image field)	(Na,Mg,Fe>Si,K,Ca) present outside impact area over ~1/2 of image field. Nothing seen in EDS.
6	15	SIMS	Mg,Si>Na,K	Na in image area all around but away from impact site; (Ca,Mg) spot in image area away from impact site.
7	60	EDS	Al,Si>Cu>Zn>S	Not analyzed in SIMS
8	15	SIMS	Na ,Mg,Si,Ca,Fe>K	(Al,Si>Na,Mg,K,Ca,Fe,Zn>Ti, Cr) spot in image field away from impact site. Nothing seen in EDS.
13	22	SIMS	Na,Mg,Si>K	(Mg,Al,Si,K,Ca,Fe) spots all around impact site
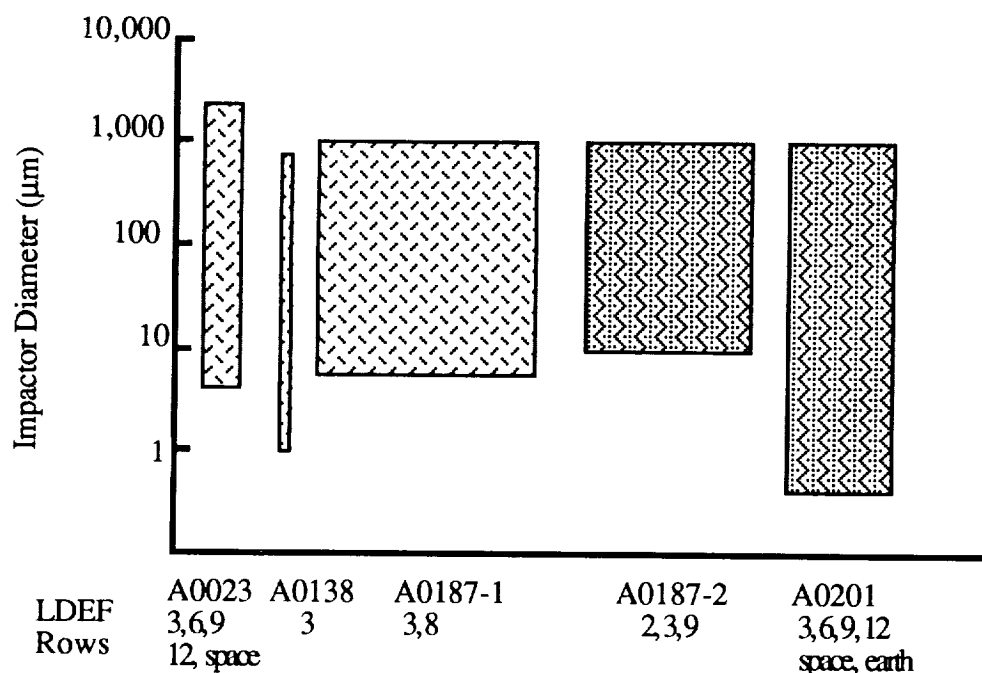
Figure 1. Range of impactor sizes characterized for LDEF micrometeoroid experiments. Width of boxes is proportional to the amount of experiment surface area exposed to space. EDS analyses = [✓] SIMS analyses = [▨]

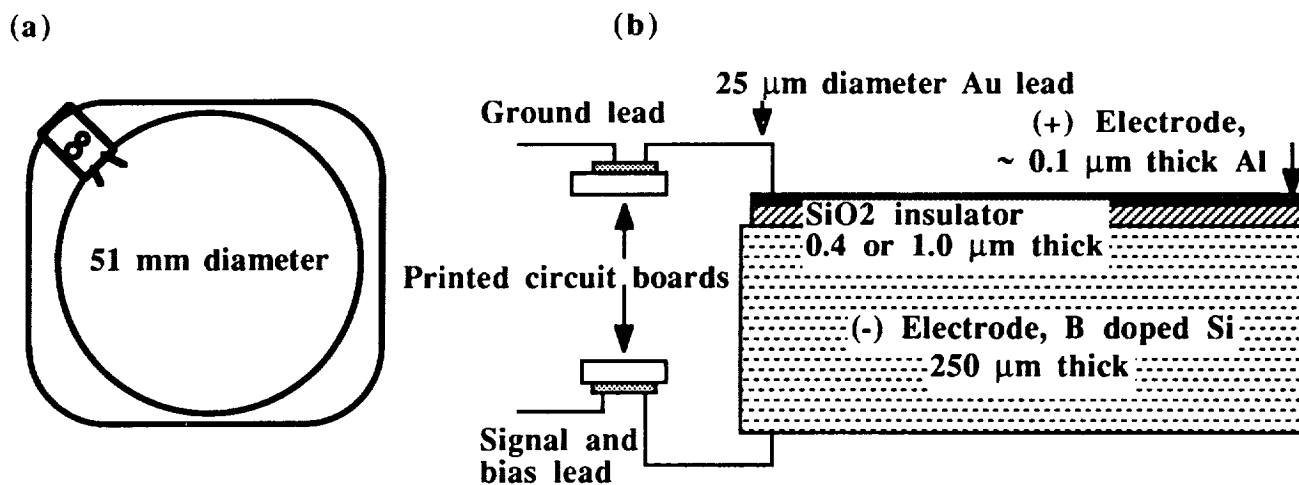**(a)**   **(b)**

Figure 2. Interplanetary Dust Experiment electro-active sensor. (a) Overall configuration of a mounted sensor. (b) Details of the electrical connections to the sensor.
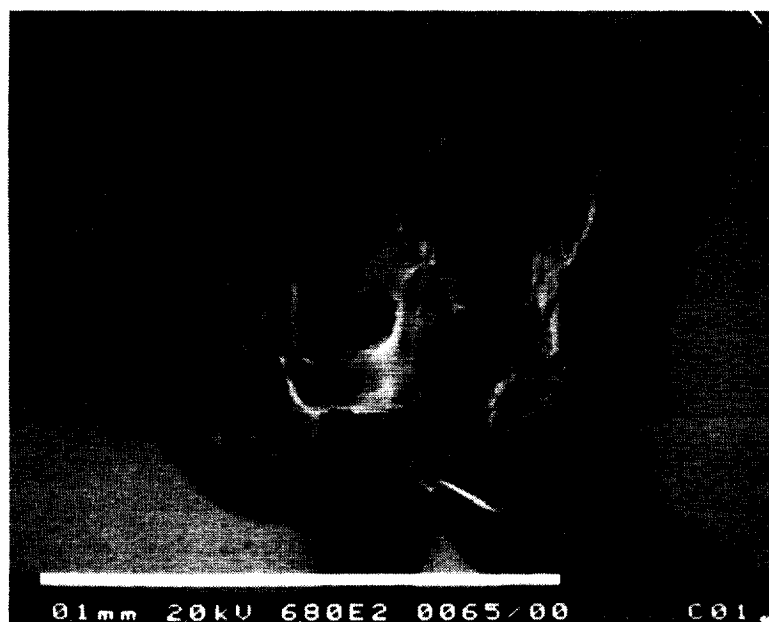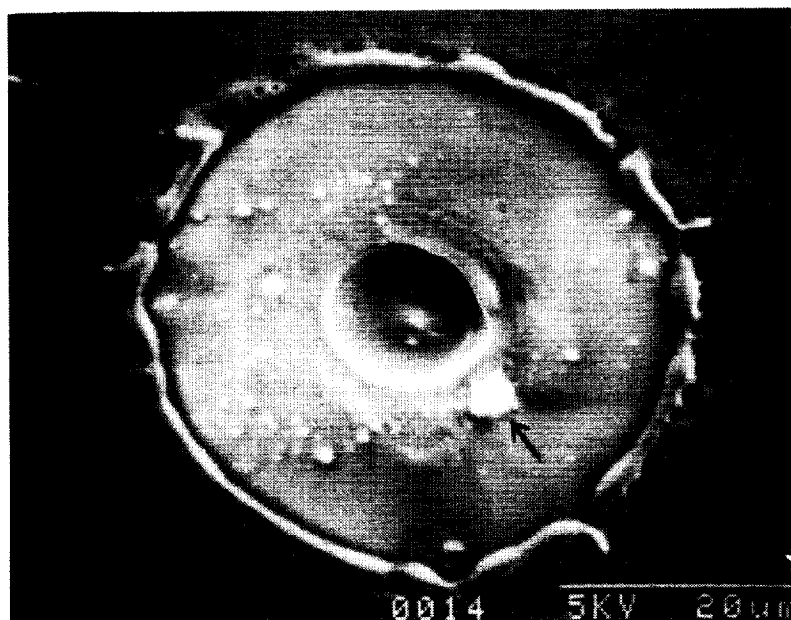
Figure 3. Small (top, No. 300-4) and large (bottom, No. 300-1) impacts on an IDE sensor . Note the four distinct morphological regions of the smaller feature: the central crater, the Al vaporization zone, the Al melt rim, and the area outside of the feature. An arrow points to a salt crystal identified in the SEM/EDS and is representative of one type of surface contamination. The larger impact feature has a spall zone that has obliterated ~1/2 of the Al vaporization zone and rim.
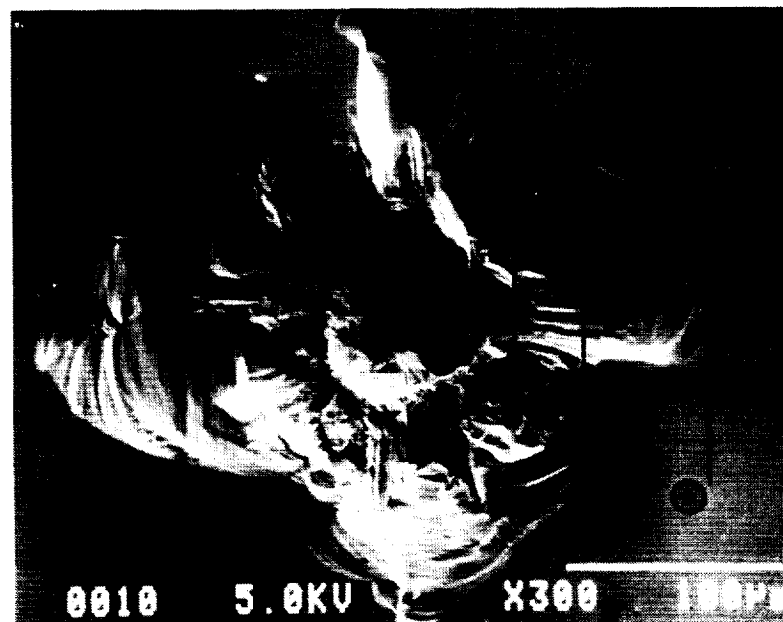
Figure 4. A small (top, Ge2B-12) and large (bottom, Ge2A-17) impact in a Ge witness plate. Note the residual hemispherical crater liner in the small impact compared to the central shatter zone in the large impact. The inner and outer spall zones are indicated on the large crater. Si and Al residue was found in the large crater with EDS, but was not indicated with SIMS presumably due to primary beam shadowing effects.
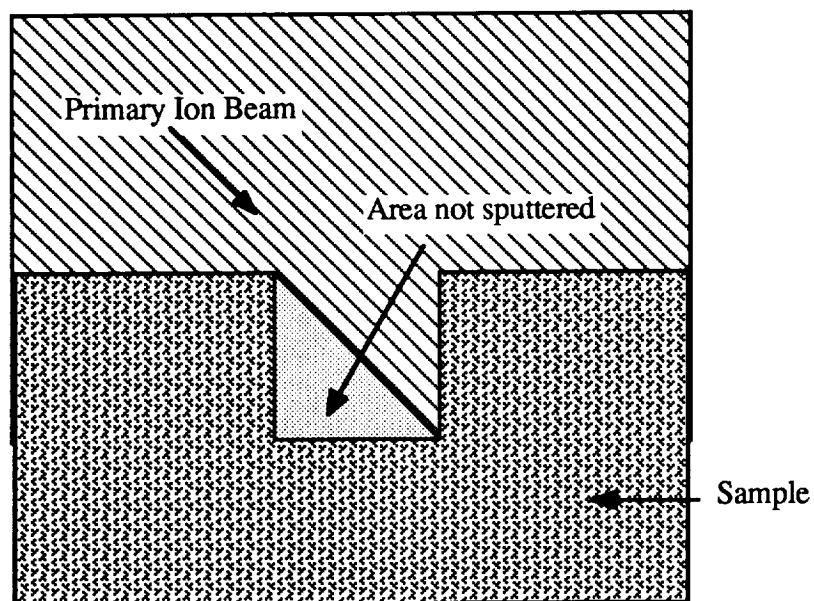
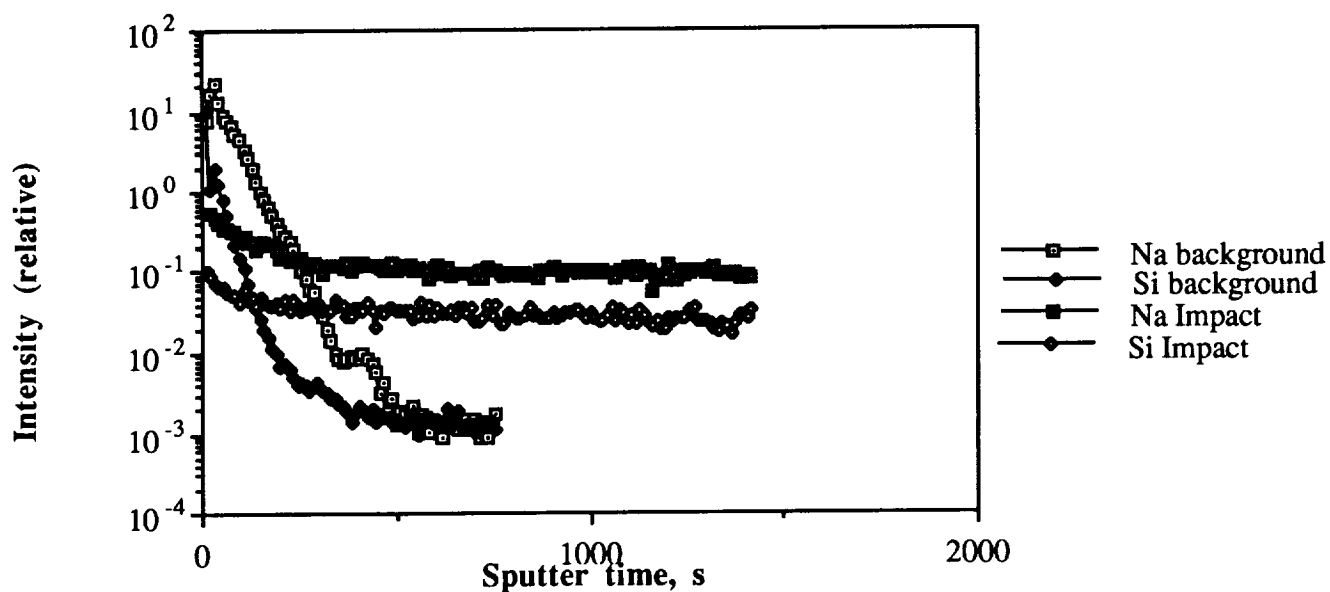Figure 5. SIMS shadowing effect on high aspect ratio features.

Figure 6. Comparison of depth profiles of the silicaceous contaminant layer over an impact feature and background area on Ge witness plate from LDEF row 12.
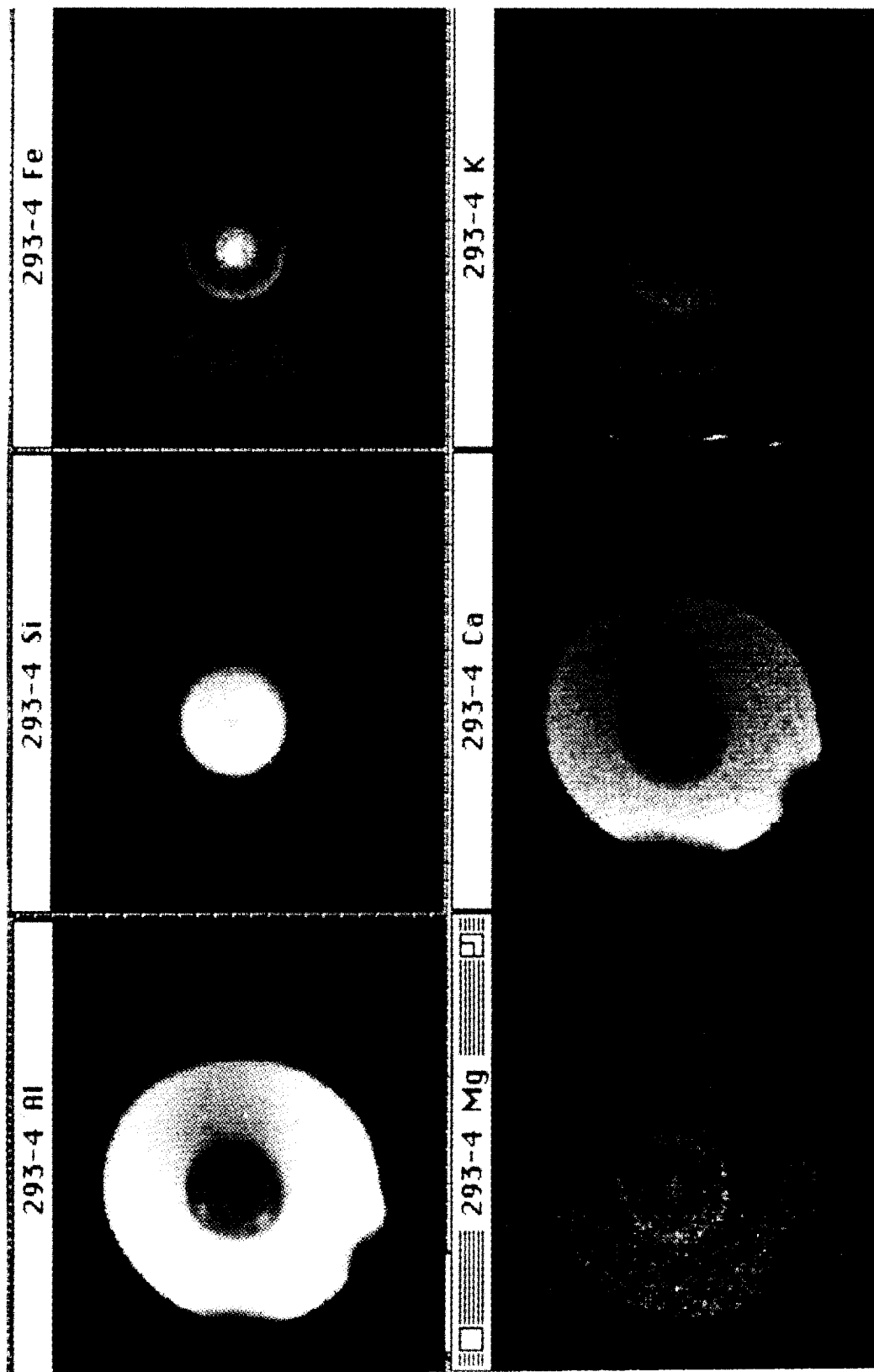
Figure 7. Unnormalized, two-dimensional positive ion images of Al+, Si+, Fe+, Mg+, Ca+ and K+ observed in impact No. 293-4. Note high Fe signal in the central crater and Fe/Mg in the feature's discharge rim. Dark areas on the right sides of all images are caused by a detector anomoly.

548